GW+*T* theory of excited electron lifetimes in metals

V. P. Zhukov, E. V. Chulkov, and P. M. Echenique
Donostia International Physics Center (DIPC), Paseo Manuel de Lardizabal, 4, 20018 San Sebastián, Spain, and Departamento de Física de Materiales and Centro Mixto CSIC-UPV/EHU, Facultad de Ciencias Químicas, Universidad del Pais Vasco/Euskal Herrico Unibertsitatea, Apdo 1072, 20018 San Sebastián/Donostia, Basque Country, Spain
(Received 19 April 2005; revised manuscript received 22 August 2005; published 12 October 2005)

We develop a first-principle *GW*+*T* approach to calculate excited electron lifetimes in metals that includes evaluation of the lowest self-energy term of the many-body perturbation theory in *GW* approximation and higher terms in the *T*-matrix approximation. The method is applied to studies of the electron lifetimes in Pd, Ta, and Al. We find that the *T*-matrix contribution to the lifetime is more important in Al than in Ta and Pd and relate this to the static screened potential. The inclusion of the *T*-matrix greatly improves agreement between experimental and theoretical results in Ta and Al.

DOI: 10.1103/PhysRevB.72.155109 PACS number(s): 71.15.−m, 78.47.+p, 79.60.−i

I. INTRODUCTION

In the last decade the de-excitation processes of photo-excited electrons in metals have been the subject of many experimental and theoretical works. The dynamics of hot electrons is fundamental for many physical phenomena such as chemical reactions on surfaces, transport, and molecular-surface interactions. The knowledge of relaxation times of electron excitations, and consequently the escape depth-length of excited electrons is important for the interpretation of photoemission spectra, Auger spectra, and low-energy electron diffraction.

Among the experimental methods developed for the studies of excited electron lifetimes the most powerful is time-resolved two-photon photoemission spectroscopy (TR-2PPE)[1] which allows the measurements directly in a time domain. A series of TR-2PPE experiments have been performed for nonmagnetic metals,[2–8] ferromagnetic metals,[9,10] and high-Tc superconductors.[11]

The key factor that influences the relaxation times in TR-2PPE experiments is the inelastic electron-electron scattering. Another process which increases the relaxation time is the effect of refilling the excited state with the cascade electrons from higher excited states. One more process that leads to the increase of the relaxation time is the Auger decay of the electrons filling excited holes. In contrast, the transport effect results in the reduction of the relaxation time due to the diffusion of electrons from irradiated spots on surface into a bulk. All such processes have been studied in Al,[12] in Ag and Au,[13] they are strongly material dependent and are not investigated yet in detail.

A number of theoretical methods have also been developed for the evaluation of lifetimes, such as semiempirical methods based on the scattering theory[10,14–16] and first-principle approaches[17] based on the self-energy formalism of many-body perturbation theory (MBPT).[18] First-principle evaluations of lifetimes have been performed for a variety of metallic systems including simple metals,[19–23] noble,[19,20,22–26] and transition metals.[21,23,27–29] Most of theoretical results have been obtained by means of the Hedin's *GW* approach of the MBPT.[30] The *GW* approach includes the lowest term of the expansion of self-energy in the powers of a screened potential *W*. Normally the calculations of the screened potential are performed in the *GW* approach within the random-phase approximation (RPA). Hence, the long-range screening, important for the quasi-particle energy, is properly accounted for. It follows, however, from a number of calculations[31] that the *GW* approach has shortcomings in describing the satellite structure in the photoemission spectra of strongly correlated systems. This structure is due to a short-range hole-hole interactions relating to the high order diagrams not included in the *GW* method.

In addition, numerous comparisons between experimental relaxation times and lifetimes obtained from the *GW* self-energy calculations have shown that, although generally the calculated lifetimes are in agreement with the trends derived from experiments, sometimes significant discrepancies are encountered. Therefore, it is important to investigate the contributions of higher terms not included in the *GW* approximation.

As follows from Hedin's formalism,[18,30–33] a natural way to improve the theory of lifetimes would be to go beyond the *GW* approach by including high-order self-energy terms. However, for real solids the calculations of all such terms are not feasible now, and normally one considers only the terms important for a problem discussed. For systems with strong electron correlation such terms are first of all the terms describing short-range correlation within the *T*-matrix formalism. Much research, based on the *T*-matrix approach and model band-structures, has been done for the self-energy and spectral properties of ferromagnetic metals.[34–37] In Ref. 38 the electron self-energy have been evaluated for ferromagnetic Fe, Co, and Ni with matrix elements adjusted to the experimental mean free path. First-principle evaluations based on the *T*-matrix theory have also been performed for magnon dispersions in Fe and Ni.[39] In Ref. 40 an *ab initio* method for the self-energy with electron-electron and hole-hole scattering has been developed and applied to the study of the photo-emission satellites in Ni.

The self-energy in the *T*-matrix approach is determined not only by multiple electron-electron and hole-hole scattering, but also by electron-hole scattering. So the approach

might be important for any system with a rather high density of states above and below the Fermi level. In this paper we expose in detail a combined first-principle $GW+T$ method which includes the GW term and the T-matrix terms and takes into account multiple electron-electron, hole-hole, and electron-hole scattering. We show the common features of the GW and T-matrix approaches and implement the method using the LMTO band-structure calculation method. A brief description of the theory together with an application to ferromagnetic Fe and Ni, has been given in Refs. 41 and 42.

The paper is organized as follows. In Sec. II the formalism of the $GW+T$ approach for the self-energy calculations is given. We discuss some fine ingredients of the approach, in particular, so-called double-counting terms and demonstrate the relations between the T-matrix self-energy and susceptibility functions. We also outline the way of calculating the excited electron lifetimes based on the $GW+T$ self-energy. In Sec. III the method is applied to the evaluation of the excited electron lifetimes in Pd, Ta, and Al. We compare the T-matrix electron-electron and electron-hole multiple contributions to lifetimes. We find that for Ta and Al the inclusion of the T-matrix greatly improves the agreement with the experiment. Unexpectedly, we come to the conclusion that the T-matrix contributions to the lifetimes are more important in free-electron-like Al than for Pd which has more localized electrons. Analyzing the main matrix elements of transverse susceptibility and screened potential, we suggest an explication of this result. In Sec. IV the obtained results are summarized.

II. THEORETICAL CONSIDERATIONS

In the framework of the many-body theory,[18,30–33,43] the lifetime of an excited electron is evaluated from the imaginary part of the self-energy expectation value. A systematic way to perform self-energy calculations is described by Hedin's equations where the self-energy is expressed in a series of terms with dynamically screened potential W as a small perturbation.[30,32] For real systems the *ab initio* calculations of all the terms are unfeasible, so one has to keep only the terms that are important for the discussed problem. In Fig. 1 we show the Feynman's diagrams for the terms of self-energy retained in our theory.

In the GW approximation one keeps for the self-energy only the first-order term in screened potential W:

$$\Sigma(1,2)_\sigma = iG_\sigma(1,2)W(1,2). \tag{1}$$

Here σ is a spin coordinate and we use short-hand notation $1 \equiv (\mathbf{r}_1, t_1)$. The details of the GW formalism and implementations are well known, see, e.g., Refs. 31 and 44. The Green's function G_σ is usually constructed from the band-states $\psi_{\mathbf{k}n\sigma}$ with energies $\epsilon_{\mathbf{k}n\sigma}$ which are most often calculated by means of the local density approximation (LDA) of the density functional theory, Ref. 45. The imaginary part of the self-energy of an excited electron, which determines the rate of de-excitation, is expressed within GW in frequency representation as

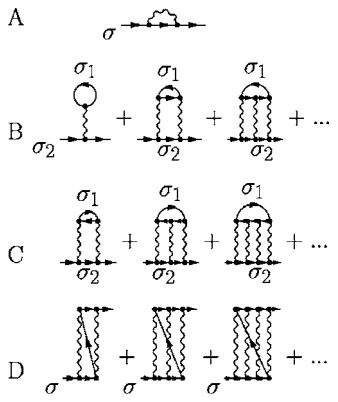

FIG. 1. Feynman diagrams for GW and T-matrix self-energy of an excited electron. A: GW-term; B: T-matrix direct terms with multiple electron-electron scattering; C: T-matrix direct terms with electron-hole scattering; D: T-matrix exchange terms. The vertical wiggly line represents static screened potential, and lines with the arrows are Green's functions. The time direction is towards the right. Changing the time direction, one obtains analogous diagrams for the self-energy of an excited hole.

$$\mathrm{Im}\,\Sigma_\sigma^{\mathrm{GW}}(\mathbf{r}_4,\mathbf{r}_2,\omega>\mu) = -\sum_{\mathbf{k}}\sum_{n}^{unocc} \psi_{\mathbf{k}n\sigma}(\mathbf{r}_4)\psi^*_{\mathbf{k}n\sigma}(\mathbf{r}_2) \times \mathrm{Im}\,W(\mathbf{r}_4,\mathbf{r}_2,\omega-\epsilon_{\mathbf{k}n\sigma})\theta(\omega-\epsilon_{\mathbf{k}n\sigma}). \tag{2}$$

We calculate the screened potential W in RPA approximation[18] that means we neglect the vertex corrections to W. As has been shown in Refs. 46 and 47, such corrections are not essential for the lifetimes calculations within the GW approach because of mutual cancellations. A basic value in our calculation is the RPA polarization, which in the frequency representation is

$$P(\mathbf{r}_4,\mathbf{r}_2,\omega) = \sum_{\sigma'}\sum_{\mathbf{k}'n'}^{occ}\sum_{\mathbf{k}''n''}^{unocc} \psi^*_{\mathbf{k}'n'\sigma'}(\mathbf{r}_4)\psi_{\mathbf{k}''n''\sigma'}(\mathbf{r}_4) \times \psi^*_{\mathbf{k}''n''\sigma'}(\mathbf{r}_2)\psi_{\mathbf{k}'n'\sigma'}(\mathbf{r}_2) \times \left\{ \frac{1}{\omega-\epsilon_{\mathbf{k}''n''\sigma'}+\epsilon_{\mathbf{k}'n'\sigma'}+i\delta} - \frac{1}{\omega+\epsilon_{\mathbf{k}''n''\sigma'}-\epsilon_{\mathbf{k}'n'\sigma'}-i\delta} \right\}. \tag{3}$$

The details of the calculations for $\mathrm{Im}\,\Sigma$ and P are given elsewhere.[19,24,25] In particular, $P(\mathbf{r}_4,\mathbf{r}_2,\omega)$ can be expanded in a basis set which consists of plane waves or products of muffin-tin orbitals. With such a basis set the matrices of polarization P and of Coulomb potential V are evaluated first. Then one calculates the matrix of the dielectric function

$$\epsilon = 1 - VP, \tag{4}$$

the matrix of the response function

$$R = (1-PV)^{-1}P, \tag{5}$$

the matrix of the inverse dielectric function

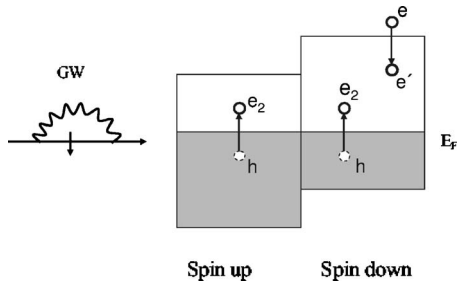

FIG. 2. Electron scattering processes included in *GW* method.

$$\epsilon^{-1} = 1 + VR \tag{6}$$

and the matrix of the screened potential

$$W = \epsilon^{-1} V. \tag{7}$$

Then the matrix Im W is expressed as

$$\text{Im } W(\omega) = V \,\text{Im } R(\omega) V. \tag{8}$$

Retaining only the largest matrix element, we have approximately

$$\text{Im } W(\omega) = V \,\text{Im } P(\omega) V / [(1 - \text{Re } P(\omega) V)^2 + (\text{Im } P(\omega) V)^2]. \tag{9}$$

So the mechanism of an excited electron decay corresponding to the *GW* approach is the following, see Fig. 2. A primary excited electron (e) with spin σ and excitation energy ω drops to one of the unoccupied states $\psi_{\mathbf{k}n\sigma}$ with the same spin and energy $\epsilon_{\mathbf{k}n\sigma}(e')$. The relaxed energy $\omega - \epsilon_{\mathbf{k}n\sigma}$ is employed to produce secondary excitations, i.e., to create electron-hole pairs (e_2 and h) corresponding to the poles of the Im R value. Usually the poles of the factor $(1 - P(\omega)V)^{-1}$, concerned with excitations of plasmons, correspond to excitation energies higher than those involved in TR-2PPE spectroscopy, therefore the contribution of this factor is negligible. So the main process responsible for the decay of excitations is the creation of electron-hole pairs in both spin channels.

In the *GW* approach the decay channel in which the final state of the primary electron has opposite spin is not included. Because of this, the secondary electron excitations with change of spin are omitted. The interactions between the electrons in the states $\psi_{\mathbf{k}n\sigma}(e')$ and the created electron-hole pairs are also disregarded.

The *T*-matrix theory incorporates some of the decay processes omitted in the *GW* approach. Within this approach, the self-energy of an excited electron includes (see Fig. 1) direct terms B of multiple scattering between the primary electron and the secondary electron of an electron-hole pair, direct terms C of scattering between the primary electron and the hole of an electron-hole pair and multiple exchange terms D. Diagrams C are essential for ferro-magnetics where they correspond to the emission of spin-waves, whereas in nearly ferro-magnetics (e.g., Pd) these diagrams are related with the creation of para-magnons. The self-energy of an excited hole also has analogous diagrams. Diagrams B for excited holes

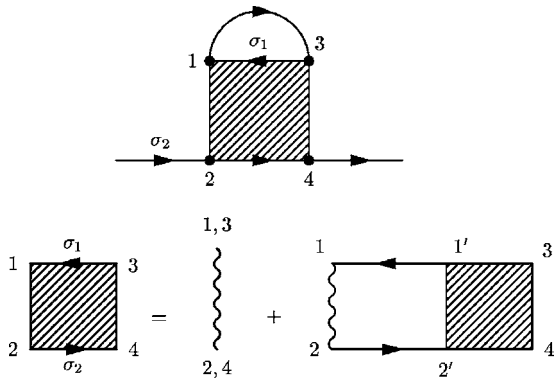

FIG. 3. Feynman diagrams for the self-energy of an electron (top figure) and for the BS equation with multiple electron-hole scattering (bottom figure). The positive time direction is to right. For the BS equation with multiple electron-electron scattering the direction of both Green's functions will be positive.

are important in explanations of the low-energy satellites in photo-emission spectra of Ni, Refs. 35, 36, and 40.

T-matrix operator is defined as a solution of the Bethe-Salpeter (BS) equation

$$T_{\sigma_1,\sigma_2}(1,2|3,4) = W(1,2)\delta(1-3)\delta(2-4) + W(1,2)\int d1'd2' K_{\sigma_1,\sigma_2}(1,2|1',2') \times T_{\sigma_1,\sigma_2}(1',2'|3,4). \tag{10}$$

Feynman's diagram for the *T*-matrix self-energy and for the BS equation are given in Fig. 3. The kernel (electron-hole propagator) of the BS equation with multiple electron-hole scattering is a product of electron and hole time-ordered Green's functions

$$K^{eh}_{\sigma_1,\sigma_2}(1,2|1',2') = iG_{\sigma_1}(1,1')G_{\sigma_2}(2',2). \tag{11}$$

For the electron-electron scattering it is a product of two electron Green functions

$$K^{ee}_{\sigma_1,\sigma_2}(1,2|1',2') = iG_{\sigma_1}(1',1)G_{\sigma_2}(2',2), \tag{12}$$

and for the hole-hole scattering it is a product of two hole Green's function

$$K^{hh}_{\sigma_1,\sigma_2}(1,2|1',2') = iG_{\sigma_1}(1,1')G_{\sigma_2}(2,2'). \tag{13}$$

With such kernels, explicit expressions for the self-energy are derived by applying usual rules.[18,32] For multiple electron-electron scattering the direct term of the self-energy is expressed as[40]

$$\Sigma^d_{\sigma_2}(4,2) = -i\sum_{\sigma_1}\int d1d3 G_{\sigma_1}(1,3)T_{\sigma_2,\sigma_1}(1,2|3,4) \tag{14}$$

whereas the exchange self-energy term is

$$\Sigma^x_{\sigma_2}(4,2) = i \int d1d3 G_{\sigma_2}(1,3) T_{\sigma_2,\sigma_2}(1,2|4,3). \quad (15)$$

For the electron-hole scattering, the Green's function in Eq. (14) is changed for $G_{\sigma_1}(3,1)$. The screened potential W is generally frequency-dependent, but we study here only low-energy excitations, so we assume for W in Eq. (10) the static approximation $W(1,2)=W(\mathbf{r}_1,\mathbf{r}_2)\delta(t_1-t_2)$. For the calculations of kernel and the T-matrix we also apply a local approximation, i.e., assume in Eqs. (11)–(13) that $1=2$ and $1'=2'$. This approximation has been proposed in Ref. 39; its validity has been confirmed by successful calculations of spin-wave energies in Fe and Ni. With such an approximation the kernels become polarization-like functions, although they depend on two spin coordinates, e.g., $K^{eh}_{\sigma_1,\sigma_2}(1,1') = iG_{\sigma_1}(1,1')G_{\sigma_2}(1',1)$. This simplifies essentially the calculations of the T-matrix which also becomes dependent only on two space and two time coordinates. The BS equation for the T-matrix is reduced to

$$T_{\sigma_1,\sigma_2}(1,2|1,2) = W(1,2) + W(1,2)K_{\sigma_1,\sigma_2}(1,2) \times T_{\sigma_1,\sigma_2}(1,2|1,2). \quad (16)$$

Besides, the calculations for self-energy are shortened. Namely, the spin-diagonal part of Σ^d with electron-electron scattering (i.e., when $\sigma_1=\sigma_2$) cancels with $\Sigma^x_{\sigma_2}$ with electron-hole scattering, so we have to calculate only the nonspin-diagonal part of Σ^d.

With such approximations, the kernel for multiple electron-hole scattering is written in frequency representation as

$$K^{eh}_{\sigma_1,\sigma_2}(1,2,\omega) = \sum_{\mathbf{k}n}^{occ}\sum_{\mathbf{k}'n'}^{unocc} \left\{ \frac{-\psi_{\mathbf{k}'n'\sigma_1}(1)\psi^*_{\mathbf{k}'n'\sigma_1}(2)\psi_{\mathbf{k}n\sigma_2}(2)\psi^*_{\mathbf{k}n\sigma_2}(1)}{\omega+\epsilon_{\mathbf{k}n\sigma_2}-\epsilon_{\mathbf{k}'n'\sigma_1}+i\delta} + \frac{\psi_{\mathbf{k}n\sigma_1}(1)\psi^*_{\mathbf{k}n\sigma_1}(2)\psi_{\mathbf{k}'n'\sigma_2}(2)\psi^*_{\mathbf{k}'n'\sigma_2}(1)}{\omega+\epsilon_{\mathbf{k}'n'\sigma_2}-\epsilon_{\mathbf{k}n\sigma_1}-i\delta} \right\}. \quad (17)$$

For multiple particle-particle (electron-electron or hole-hole) scattering it is[40]

$$K^{pp}_{\sigma_1,\sigma_2}(1,2,\omega) = \sum_{\mathbf{k}n}^{unocc}\sum_{\mathbf{k}'n'}^{unocc} \frac{\psi_{\mathbf{k}n\sigma_1}(2)\psi^*_{\mathbf{k}n\sigma_1}(1)\psi_{\mathbf{k}'n'\sigma_2}(2)\psi^*_{\mathbf{k}'n'\sigma_2}(1)}{\omega-\epsilon_{\mathbf{k}n\sigma_1}-\epsilon_{\mathbf{k}'n'\sigma_2}+i\delta} - \sum_{\mathbf{k}n}^{occ}\sum_{\mathbf{k}'n'}^{occ} \frac{\psi_{\mathbf{k}n\sigma_1}(2)\psi^*_{\mathbf{k}n\sigma_1}(1)\psi_{\mathbf{k}'n'\sigma_2}(2)\psi^*_{\mathbf{k}'n'\sigma_2}(1)}{\omega-\epsilon_{\mathbf{k}n\sigma_1}-\epsilon_{\mathbf{k}'n'\sigma_2}-i\delta}. \quad (18)$$

Here the sum over unoccupied states corresponds to the electron-electron scattering ($pp=ee$), and the sum over occupied states is for hole-hole scattering ($pp=hh$).

Practically, we calculate first the spectral function of the kernel that is expressed for electron-hole scattering as

$$S^{eh}_{\sigma_1,\sigma_2}(1,2,\omega) = \sum_{\mathbf{k}n}^{occ}\sum_{\mathbf{k}'n'}^{unocc} \{\psi_{\mathbf{k}'n'\sigma_1}(1)\psi^*_{\mathbf{k}'n'\sigma_1}(2)\psi_{\mathbf{k}n\sigma_2}(2)\psi^*_{\mathbf{k}n\sigma_2}(1)\delta(\omega+\epsilon_{\mathbf{k}n\sigma_2}-\epsilon_{\mathbf{k}'n'\sigma_1}) - \psi_{\mathbf{k}n\sigma_1}(1)\psi^*_{\mathbf{k}n\sigma_1}(2)\psi_{\mathbf{k}'n'\sigma_2}(2)\psi^*_{\mathbf{k}'n'\sigma_2}(1) \times \delta(\omega+\epsilon_{\mathbf{k}'n'\sigma_2}-\epsilon_{\mathbf{k}n\sigma_1})\} \quad (19)$$

and for particle-particle scattering as

$$S^{pp}_{\sigma_1,\sigma_2}(1,2,\omega) = -\sum_{\mathbf{k}n}^{unocc}\sum_{\mathbf{k}'n'}^{unocc} \psi_{\mathbf{k}n\sigma_1}(2)\psi^*_{\mathbf{k}n\sigma_1}(1)\psi_{\mathbf{k}'n'\sigma_2}(2)\psi^*_{\mathbf{k}'n'\sigma_2}(1)\delta(\omega-\epsilon_{\mathbf{k}n\sigma_1}-\epsilon_{\mathbf{k}'n'\sigma_2}) + \sum_{\mathbf{k}n}^{occ}\sum_{\mathbf{k}'n'}^{occ} \psi_{\mathbf{k}n\sigma_1}(2)\psi^*_{\mathbf{k}n\sigma_1}(1)\psi_{\mathbf{k}'n'\sigma_2}(2)\psi^*_{\mathbf{k}'n'\sigma_2}(1)\delta(\omega-\epsilon_{\mathbf{k}n\sigma_1}-\epsilon_{\mathbf{k}'n'\sigma_2}). \quad (20)$$

Spectral function $S^{eh}_{\sigma_1,\sigma_2}(\omega)$ gives the probability of all the electrons transitions between occupied states with spin σ_1 and unoccupied states with spin σ_2 at the energy of transitions equal to ω. Function $S^{pp}_{\sigma_1,\sigma_2}(\omega)$ gives the probability of all the electron (hole) excitations with spin σ_1 and all the electron (hole) excitations with spin σ_2, such that the energy of both excitations is equal to ω. The kernel is calculated through Hilbert transform

$$-K_{\sigma_1,\sigma_2}(1,2,\omega) = \mathcal{P}\int d\omega' \frac{S_{\sigma_1,\sigma_2}(1,2,\omega')}{(\omega-\omega')} - i\pi S_{\sigma_1,\sigma_2}(1,2,\omega)sgn(\omega). \quad (21)$$

Equations for the imaginary part of the T-matrix self-energy are derived in the way similar to that employed in the GW approach.[40,44] For an excited electron with multiple electron-

hole scattering we obtain in the local approximation

$$\mathrm{Im}\,\Sigma^{d}_{\sigma_2}(\mathbf{r}_4,\mathbf{r}_2,\omega>\mu) = -\sum_{\sigma_1}\sum_{\mathbf{k}}\sum_{n'}^{unocc}\psi_{\mathbf{k}n'\sigma_1}(\mathbf{r}_4)\psi^{*}_{\mathbf{k}n'\sigma_1}(\mathbf{r}_2) \times \mathrm{Im}\,T^{eh}_{\sigma_2,\sigma_1}(\mathbf{r}_2,\mathbf{r}_4,\omega-\epsilon_{\mathbf{k}n'\sigma_1})\theta(\omega-\epsilon_{\mathbf{k}n'\sigma_1}) \quad (22)$$

and for an excited hole with electron-hole scattering we have

$$\mathrm{Im}\,\Sigma^{d}_{\sigma_2}(\mathbf{r}_4,\mathbf{r}_2,\omega<\mu) = \sum_{\sigma_1}\sum_{\mathbf{k}}\sum_{n}^{occ}\psi_{\mathbf{k}n\sigma_1}(\mathbf{r}_4)\psi^{*}_{\mathbf{k}n\sigma_1}(\mathbf{r}_2) \times \mathrm{Im}\,T^{eh}_{\sigma_2,\sigma_1}(\mathbf{r}_2,\mathbf{r}_4,\omega-\epsilon_{\mathbf{k}n\sigma_1})\theta(\epsilon_{\mathbf{k}n\sigma_1}-\omega). \quad (23)$$

For en excited electron with multiple electron-electron scattering we have[40]

$$\mathrm{Im}\,\Sigma^{d}_{\sigma_2}(\mathbf{r}_4,\mathbf{r}_2,\omega>\mu) = \sum_{\sigma_1}\sum_{\mathbf{k}}\sum_{n}^{occ}\psi_{\mathbf{k}n\sigma_1}(\mathbf{r}_2)\psi^{*}_{\mathbf{k}n\sigma_1}(\mathbf{r}_4) \times \mathrm{Im}\,T^{ee}_{\sigma_2\sigma_1}(\mathbf{r}_2,\mathbf{r}_4,\omega+\epsilon_{\mathbf{k}n\sigma_1})\theta(\omega+\epsilon_{\mathbf{k}n\sigma_1}-2\mu) \quad (24)$$

and for an excited hole with multiple hole-hole scattering we have

$$\mathrm{Im}\,\Sigma^{d}_{\sigma_2}(\mathbf{r}_4,\mathbf{r}_2,\omega<\mu) = -\sum_{\sigma_1}\sum_{\mathbf{k}}\sum_{n'}^{unocc}\psi_{\mathbf{k}n'\sigma_1}(\mathbf{r}_2)\psi^{*}_{\mathbf{k}n'\sigma_1}(\mathbf{r}_4) \times \mathrm{Im}\,T^{hh}_{\sigma_2\sigma_1}(\mathbf{r}_2,\mathbf{r}_4,\omega+\epsilon_{\mathbf{k}n'\sigma_1})\theta(-\omega-\epsilon_{\mathbf{k}n'\sigma_1}+2\mu). \quad (25)$$

In Fig. 4 we illustrate the processes included in the *T*-matrix theory. Figures 4(a) and 4(b) depict the processes with multiple electron-hole scattering whereas the bottom figure [Fig. 4(c)] refers to multiple electron-electron scattering. In Figs. 4(a) and 4(b) a primary electron (e) with spin σ_2 and excitation energy ω drops to an unoccupied state (e_2) with the same spin and a lower energy $\epsilon_{\mathbf{k}n'\sigma_2}$. The relaxed energy is used to create an electron-hole pair (e_1-h) in the same or in the opposite spin channel. The interaction between the primary and secondary electrons is absent here; it is included in Fig. 4(c). The energy $\omega-\epsilon_{\mathbf{k}n'\sigma_2}$ belongs to an interacting electron-hole pair e_2-h. The secondary excitations with this energy are concerned with the poles of the value $\mathrm{Im}\,T(\omega-\epsilon_{\mathbf{k}n'\sigma_1})$. According to Eq. (16), the *T*-matrix is expressed in frequency representation as

$$T_{\sigma_1,\sigma_2}(\omega) = [1-WK_{\sigma_1,\sigma_2}(\omega)]^{-1}W. \quad (26)$$

If we define susceptibilities

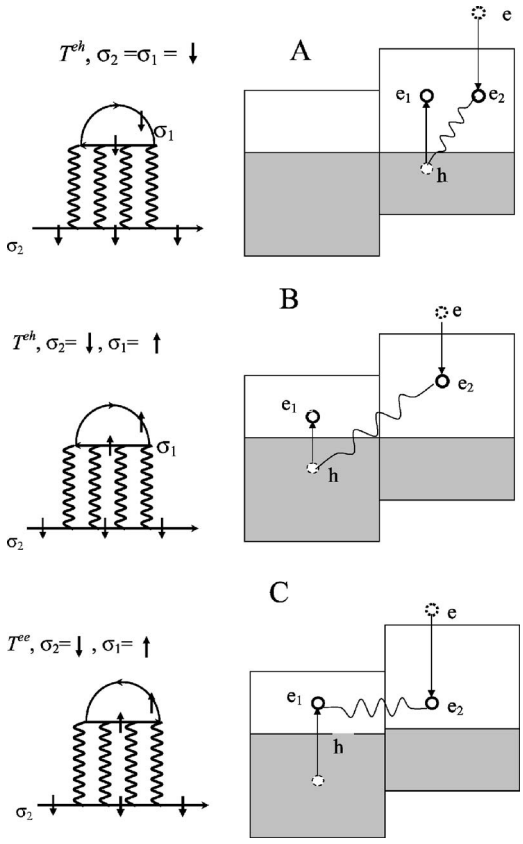

FIG. 4. Electrons scattering processes included in the *T*-matrix theory. In the right column with zigzag line we connect the particles with multiple scattering. In the left column we show Feynman diagrams for the illustrated processes.

$$R_{\sigma_1,\sigma_2} = K_{\sigma_1,\sigma_2}[1-WK_{\sigma_1,\sigma_2}]^{-1} \quad (27)$$

then

$$\mathrm{Im}\,T_{\sigma_1,\sigma_2}(\omega) = W\,\mathrm{Im}\,R_{\sigma_1,\sigma_2}(\omega)W. \quad (28)$$

If we approximate the matrices by their main matrix elements, we have

$$\mathrm{Im}\,R_{\sigma_1,\sigma_2} = \mathrm{Im}\,K_{\sigma_1,\sigma_2}/[(1-W\,\mathrm{Re}\,K_{\sigma_1,\sigma_2})^2+(W\,\mathrm{Im}\,K_{\sigma_1,\sigma_2})^2]. \quad (29)$$

So the contributions of the *T*-matrix to $\mathrm{Im}\,\Sigma$ are determined by the longitudinal $R_{\sigma,\sigma}$ and transverse $R_{\sigma,-\sigma}$ susceptibilities. For cubic paramagnetic crystals these susceptibilities are equal. It follows from Eq. (27) that the susceptibilities may have two types of poles. The poles of $\mathrm{Im}\,K_{\sigma_1,\sigma_2}$ correspond to the creation of electron-hole pairs with the holes in the spin channel σ_2 and the electrons in the channel σ_1. So, in contrast to *GW*, such excitations occur both without the change of spin, Fig. 4(a), and with the change of spin, Fig. 4(b). The conservation of total spin moment is evident in Fig. 4(a). In Fig. 4(b) the creation of electron-hole pairs is accompanied by the change of spin equal to $-\hbar$. But the disappearance of the electron e and appearance of the electron e_1 corresponds to the change of spin equal to $\hbar$, so the total spin moment is also conserving.

An essential difference with *GW* is that at low frequencies the poles of the value $[1-WK]^{-1}$, usually called a susceptibility enhancement factor, can be important. This is the case of ferro-magnetics where the value $\mathrm{Im}\, R_{-1/2,1/2}$ is recognized as the spectral function of spin-waves excitations. For example, the *ab initio* calculations for Fe[41] show that at magnon energies the factor $[1-WK]^{-1}$ is big and the *T*-matrix term in $\mathrm{Im}\,\Sigma$ is bigger than the *GW* term. So the main loss of energy of a hot electron in Fe, if the energy is less than 0.5 eV, is concerned with the excitations of magnons. At the excitation energy above 1 eV the spin-diagonal *T*-matrix contributions become also important. In the following we will show that the *T*-matrix terms with multiple electron-hole scattering provide also a noticeable contributions into the self-energy of paramagnetic Pd, Ta, and Al.

Figure 4(c) illustrates the multiple scattering between the primary electron e_2 and the secondary electron e_1 of an electron-hole pair. Whereas the kernel of multiple electron-hole scattering depends on the occupied and empty states, the kernel of electron-electron scattering is determined only by the convolution of the density of empty states. We will show later that the electron-electron scattering is important in Al.

One fine question concerns the problem of double counting terms (DCT) in the *GW+T* approach. A thorough analysis of the Hedin's formalism shows that the direct term of the second order in *W* is absent.[32] In the *GW+T* approach such term, with a static potential, is included in the *T*-matrix series in order to make it complete. It has been shown in Ref. 40 that a simple subtraction of the second-order term leads to un-physical negative spectral function. We also found that the subtraction of the second-order term, calculated with polarization function as in Fig. 1, yields un-physical negative contributions to lifetimes. So we calculate DCT with the polarization function replaced by the response function; for the argumentation we refer the reader to Ref. 40. Within the adopted approximations the DCT is expressed as

$$\mathrm{Im}\,\Sigma^{D(R)}_{\sigma_2}(\mathbf{r}_4,\mathbf{r}_2,\omega>\mu) = \sum_{\mathbf{k}}\sum_{n'}^{unocc} \psi_{\mathbf{k}n'\sigma_2}(\mathbf{r}_4)\psi^{*}_{\mathbf{k}n'\sigma_2}(\mathbf{r}_2) \times \mathrm{Im}\, D(\mathbf{r}_4,\mathbf{r}_2,\omega-\epsilon_{\mathbf{k}n'\sigma_2})\,\theta(\omega-\epsilon_{\mathbf{k}n'\sigma_2}), \quad (30)$$

$$\mathrm{Im}\,\Sigma^{D(R)}_{\sigma_2}(\mathbf{r}_4,\mathbf{r}_2,\omega<\mu) = -\sum_{\mathbf{k}}\sum_{n}^{occ} \psi_{\mathbf{k}n\sigma_2}(\mathbf{r}_4)\psi^{*}_{\mathbf{k}n\sigma_2}(\mathbf{r}_2) \times \mathrm{Im}\, D(\mathbf{r}_4,\mathbf{r}_2,\epsilon_{\mathbf{k}n\sigma_2}-\omega)\,\theta(\epsilon_{\mathbf{k}n\sigma_2}-\omega), \quad (31)$$

where

$$D(\mathbf{r}_4,\mathbf{r}_2,\omega) = \int d^3r_1 d^3r_3 W(\mathbf{r}_2,\mathbf{r}_1)R(\mathbf{r}_1,\mathbf{r}_3,\omega)W(\mathbf{r}_3,\mathbf{r}_4). \quad (32)$$

It cancels the double counting in the *GW* and *T*-matrix with electron-hole scattering. When the *T*-matrix with multiple electron-electron scattering is also included, we have to cancel again the direct second-order term in *W*. Taking into account that the exchange *T*-matrix term cancels the spin-diagonal part of the direct *T*-matrix term with electron-electron scattering, the second DCT, $\mathrm{Im}\,\Sigma^{D(P)}$, is similar to that in Eqs. (30)–(32), with response function *R* replaced by polarization function *P* and divided by 2. Since the electron-electron scattering is big only in Al, we evaluate the second DCT only for Al.

The direct first-order term is included in the *T*-matrix series also formally, see p. 134 of Ref. 33. It is absent in the Hedin's equations for self-energy, so it has to be also subtracted. But with the static approximation for screened potential this term does not produce a contribution to the imaginary part of self-energy, so it is irrelevant for lifetime calculation. Hence, in the *GW+T* approach the lifetime is calculated from $\mathrm{Im}\,\Sigma^{GW+T}=\mathrm{Im}\,\Sigma^{GW}+\mathrm{Im}\,\Sigma^{T}-\mathrm{Im}\,\Sigma^{D(R)}-\mathrm{Im}\,\Sigma^{D(P)}$. The inverse lifetime is defined by the complex quasi-particle energy $E_{\mathbf{q}n}(\omega)$ which is obtained from the Dyson's equation

$$E_{\mathbf{q}n\sigma}(\omega) = \epsilon_{\mathbf{q}n\sigma} + \langle\psi_{\mathbf{q}n\sigma}|\Delta\Sigma_{\sigma}(\omega)|\psi_{\mathbf{q}n\sigma}\rangle. \quad (33)$$

Here $\Delta\Sigma_{\sigma}(\omega)=\Sigma_{\sigma}(\omega)-V^{xc}_{\sigma}(\mathrm{LDA})$, with $V^{xc}_{\sigma}(\mathrm{LDA})$ being LDA exchange-correlation potential, provides many-body corrections to the LDA eigenvalues $\Delta\epsilon_{\mathbf{q}n\sigma}=E_{\mathbf{q}n\sigma}-\epsilon_{\mathbf{q}n\sigma}$. We solve the equation by employing the re-normalization factor of Green's function *Z*[18]

$$Z_{\mathbf{q}n\sigma} = \left[1-\frac{\partial\,\mathrm{Re}\,\Delta\Sigma_{\mathbf{q}n\sigma}(\omega)}{\partial\omega}\right]^{-1}_{\omega=\epsilon_{\mathbf{q}n\sigma}}. \quad (34)$$

As usual, we neglect the imaginary part of *Z*. Finally, the imaginary part of $\Delta\epsilon_{\mathbf{q}n\sigma}$ determines the inverse of a quasi-particle lifetime (line-width):

$$\tau^{-1}_{\mathbf{q}n\sigma} = 2\times|\mathrm{Im}\,\Delta\epsilon_{\mathbf{q}n\sigma}|, \quad (35)$$

where $\mathrm{Im}\,\Delta\epsilon_{\mathbf{q}n}=Z_{\mathbf{q}n\sigma}\times\langle\psi_{\mathbf{q}n\sigma}|\Delta\Sigma(\epsilon_{\mathbf{q}n\sigma})|\psi_{\mathbf{q}n\sigma}\rangle$.

We perform LDA band-structure calculations in the basis of linear muffin-tin-orbitals[48] (LMTO), and many-body calculations in the basis of LMTO product-orbitals.[31,44] The details of the RPA calculations for screened potential *W* are similar to those for Nb, Mo, Rh, and Pd.[27] The number of momentum vectors in full Brillouin zone is equal to 8000. The band structure is calculated with the minimal s,p,d-basis set, whereas the basis set of many-body calculations consists of orthogonalized linear combinations of the $s\times s$, $s\times p$, $s\times d$, $p\times p$, $p\times d$, $d\times d$ products of LMTO's. The total number of the product basis function is typically 40–45. The first, most important product basis function has the composition $|1\rangle=C_1|ss\rangle+C_2\Sigma_i|p_ip_i\rangle+C_3\Sigma_j|d_jd_j\rangle$, where s, p_i, d_j are all the inter-sphere parts of the *s*-, *p*-, and *d*-LMTO's. For Pd the *C*-values are equal to 0.27, 0.27, 0.95; for Ta and Al they are 1.05, 1.20, 1.20 and 1.08, 1.13, 1.20, respectively. One of the virtues of such basis set is that the matrix elements $\langle1|S|1\rangle$, $\langle1|K|1\rangle$, $\langle1|(1-WK)^{-1}|1\rangle$, i.e., over the first basis function, are much larger than the rest of the matrix elements. So below we discuss these first matrix elements which helps us in making our results more transparent. In the calculations of spectral func-

tions we replace the delta-functions in Eqs. (19) and (20) with the Gaussians of the width 0.136 eV (0.005 Hartree a.u.). The Hilbert transform from imaginary to the real part of self-energy, Eq. (21), is performed numerically with the step of frequency also equal to 0.136 eV.

III. THE SPIN-SPIN DENSITY CORRELATION FUNCTIONS AND QUASI-PARTICLE LIFETIMES IN PD, TA, AND AL

Our choice of the materials under study is based on the following reasons. First is that Pd, Ta, and Al are the species whose electron lifetimes have been most extensively investigated. In Refs. 27–29 theoretical studies of the electron lifetimes in Pd have been performed within the *GW* approach. In Ref. 29 the calculated lifetimes in Pd have also been used to simulate the experiments on ballistic electron emission spectroscopy. A good correspondence between the data of Refs. 27–29 confirms the reliability of the *GW* evaluations. Notice also that the dynamic susceptibility in Pd, a quantity associated with lifetimes, has been extensively studied before—see references in the Pd subsection. The electron lifetimes in Ta have been recently obtained from the TR-2PPE measurements.[49] The electron lifetimes in Al have been deduced in Ref. 13 from the TR-2PPE experiments; the effects of transport and secondary Auger electrons have also been studied. The electron lifetimes in Al have been calculated with the *GW* method in Refs. 19 and 27.

Secondly, Pd, Ta, and Al have very different electronic structures. In Fig. 5 we illustrate this by showing the densities of states. The primary excited electrons in Pd occupy free-electron like states. The secondary electron excitations, associated with polarization function, mainly occur between occupied *d*-states and free-electron-like states. Palladium is a material with well expressed correlation effects, which is confirmed by the high calculated value of the susceptibility enhancement factor equal to 4.46, see Ref. 50. In Ta the primary excited electrons occupy *d*-states. The polarization in Ta is related with the excitations between occupied and empty *d*-states. The width of the *d*-bands in Ta (6 eV) is bigger than in Pd (3 eV), and the density of states at the Fermi level is much lower. Therefore, the correlation effects in Ta are less expressed, that corresponds to the lower value of the enhancement factor, 1.50, see Ref. 51. Aluminum is a typical free-electron-like metal with low density of states. So the correlation effects in Al are less pronounced than in Ta, and the calculated susceptibility enhancement factor is equal to 1.34, see Ref. 50. In Pd and Ta the density of states above Fermi level is less than that below E_F. So, according to Eqs. (19) and (20), one may expect than the effects of electron-hole scattering are in Pd and Ta less important comparing with electron-electron scattering. In Al, contrary to Pd and Ta, the density of states above the Fermi level is higher than that below E_F, so one may expect that the multiple electron-electron scattering is stronger.

Hence, investigating Pd, Ta, and Al, one can get a broad insight into the role of the three self-energy terms, i.e., the *GW*-, the *T*-, and the double counting terms. One can also compare the effects of electron-electron and electron-hole multiple scattering and reveal the features of electronic structure associated with the contributions of all the terms in the decay rate of excited electrons.

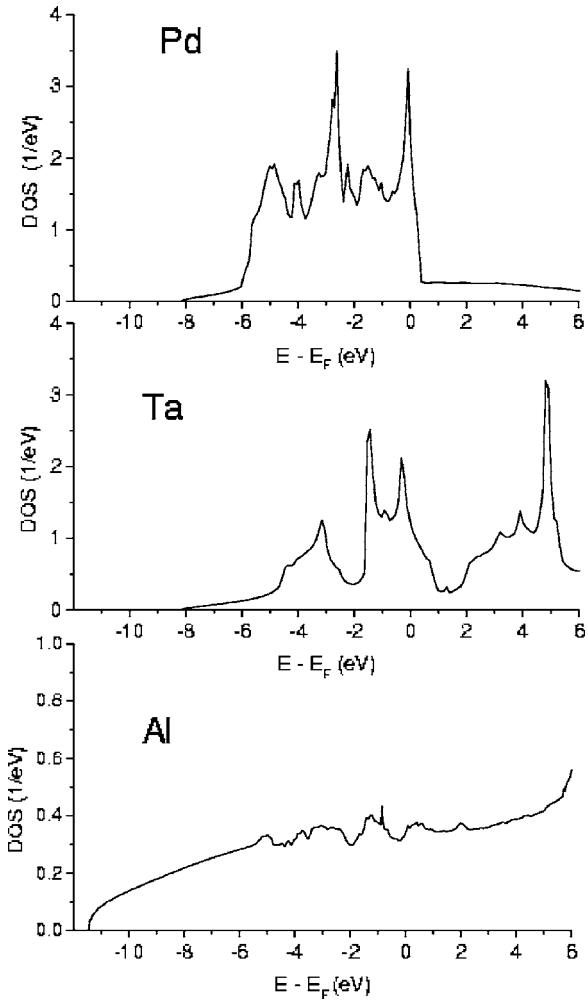

FIG. 5. Total density of states in Pd, Ta, Al.

A. Pd

Palladium belongs to an interesting class of nearly ferromagnetic materials, and a great amount of experimental and theoretical studies has been performed for its properties. An intriguing phenomenon in Pd is the low-temperature anomaly of specific heat concerned with the existence of paramagnon excited states.[52] The electronic structure and spin susceptibilities in Pd associated with this anomaly were studied in many *ab initio* researches. The static susceptibility has been evaluated in Refs. 51, 53, and 54; the dynamic susceptibility has been studied in Refs. 55–57. As follows from model and first-principle calculations,[38,42] the generation of magnons in ferromagnetic materials can essentially decrease lifetimes of excited electrons. So a question arises if such effect can exist in nearly ferromagnetic materials with paramagnon excited states.

The existence of paramagnon excited states is associated with the peculiarities of the spectral function of the electron-hole kernel, Eq. (18). In Fig. 6 we show the frequency and

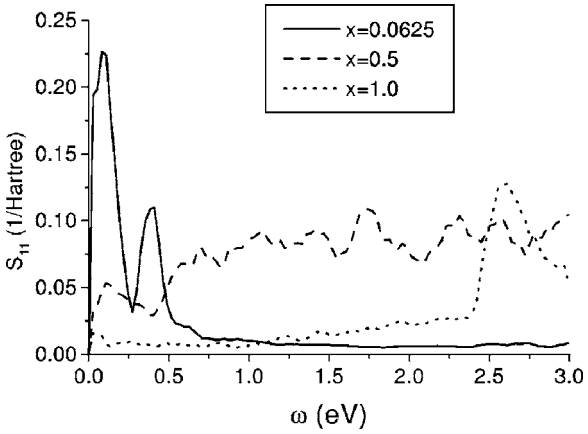

FIG. 6. Frequency dependence of the main matrix element of Pd spectral function at three points $q=(2\pi/a)(x,0,0)$ of the Brillouin zone.

momentum dependence of the main matrix element of this spectral function. At small momentum **q** it has a well-defined peak with maximum at frequency about 0.1 eV; the peak speedily broadens with increasing **q**. In Fig. 7 we show the dispersion curves of electrons in Pd that help to conclude that the given peak belongs to a set of direct transitions from the highest occupied to the lowest unoccupied band in the points around X. The amplitude of the peak is much lower than that of the $d-d$ spin-flip excitations responsible for the magnon generation in ferromagnetics,[41] nevertheless it essentially affects the low-energy excited states. The spin-flip excitation spectrum is derived from the spectral function of the spin-spin density correlation function

$$R^{-+}(1,2) = -i\langle T\sigma^{-}(1)\sigma^{+}(2)\rangle, \tag{36}$$

where $\sigma^{+}=\sigma_x+i\sigma_y$ and $\sigma^{-}=\sigma_x-i\sigma_y$. The calculations of the R^{-+} function with model band structures were discussed in many publications see, e.g., Ref. 52. Here we follow the method of the first-principle calculations exposed in Refs. 39 and 58. At low temperature the value R^{-+} can be expressed as

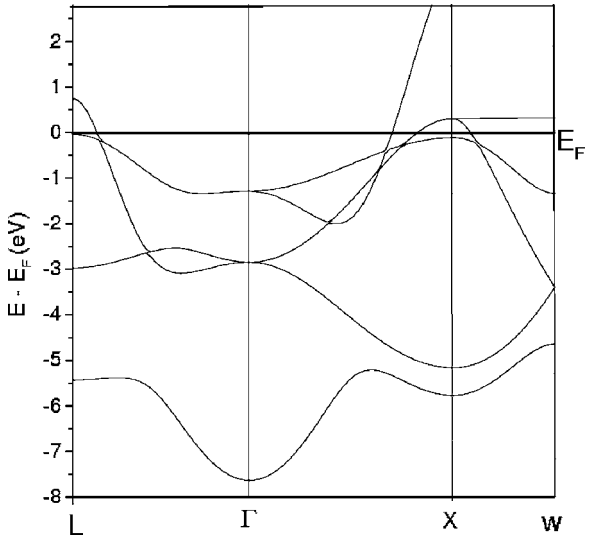

FIG. 7. Electron energy band structure in Pd.

$$R^{-+} = [1 + K_{-1/2,1/2}T_{-1/2,1/2}]K_{-1/2,1/2}. \tag{37}$$

So at low temperature the value R^{-+} coincides with the transverse susceptibility $R_{-1/2,1/2}$, Eq. (27). We can represent R^{-+} as a sum $R^{-+}=R_K^{-+}+R_T^{-+}$ where

$$R_K^{-+} = K_{-1/2,1/2} \tag{38}$$

and

$$R_T^{-+} = K_{-1/2,1/2}[1 - WK_{-1/2,1/2}]^{-1}WK_{-1/2,1/2}. \tag{39}$$

The value $\mathrm{Im}\,R_K^{-+}$ shows the part of the excitation spectra that belongs to the creation of electron-hole pairs whereas the $\mathrm{Im}\,R_T^{-+}$ shows the enhancement of the spectra due to the collective effects, i.e., paramagnons. In Fig. 8 we show the values R^{-+}, R_K^{-+}, R_T^{-+} in the point of the Brillouin zone $q=(2\pi/a)(0.0625,0,0)$ which is in our calculations the closest to Γ. Qualitatively, these results are in agreement with the previous calculations[56,57] performed within the time-dependent density functional theory. As in Ref. 56, we ob-

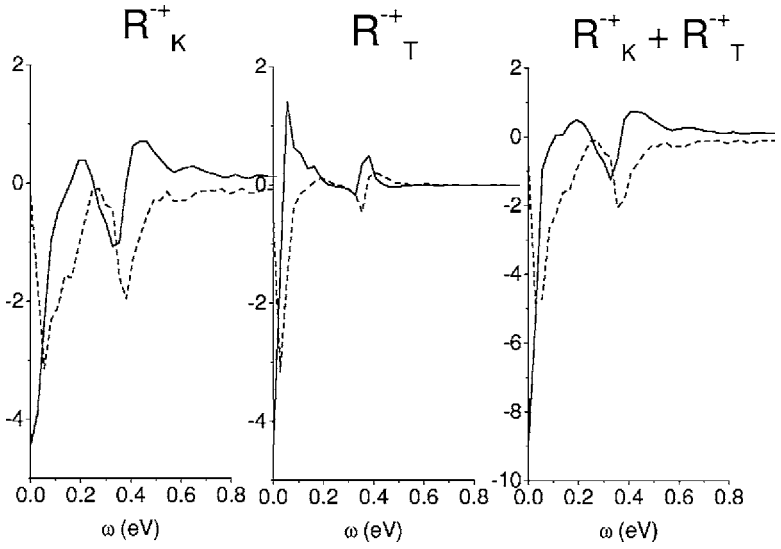

FIG. 8. Components of the transverse susceptibility in Pd. Solid line: Real part of R^{-+}; dashed line: Imaginary part of R^{-+}. $q=(2\pi/a)(0.0625,0,0)$.

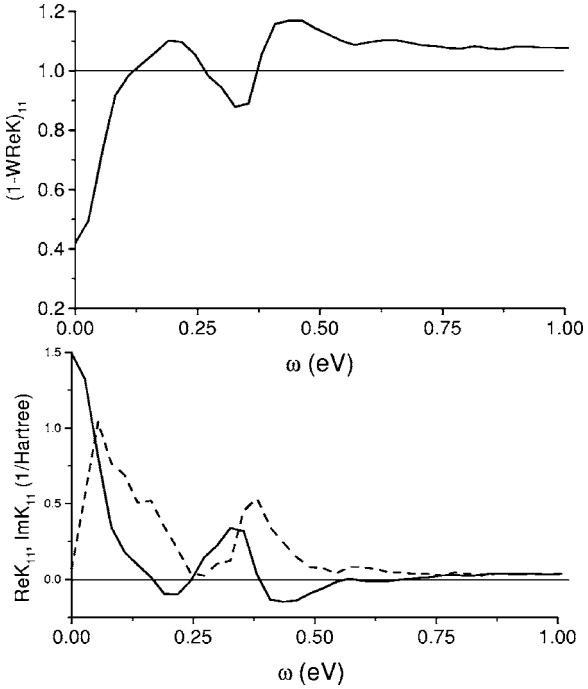

FIG. 9. Top panel: Frequency dependence of the main matrix element of the inverse enhancement factor $(1-W\,\mathrm{Re}\,K)_{11}$ in Pd. Bottom panel: Imaginary part (dashed line) and real part (solid line) of the main matrix element of electron-hole kernel in Pd. $q=(2\pi/a)(0.0625,0,0)$.

serve two minima of the value $\mathrm{Im}\,R_K^{-+}$ at frequencies about 0.1 and 0.4 eV which are concerned with two peaks in the spectral function of the kernel, Fig. 6. The $\mathrm{Im}\,R_T^{-+}$ shows a dip with the minimum at 0.05 eV. So the *T*-matrix contribution markedly enhances the spectral function of R^{-+} and shifts it to lower frequency. This leads, through the Hilbert transform, to an about two-times enhancement of the static susceptibility.

In Fig. 9 we show the frequency dependence of the main matrix elements of the inverse enhancement factor $(1-W\,\mathrm{Re}\,K)_{11}$ and of the quantities $\mathrm{Im}\,K_{11}=\pi S_{11}$, $\mathrm{Re}\,K_{11}$. Due to the presence of the low-frequency peak in $\mathrm{Im}\,K$, its Hilbert-transform, $\mathrm{Re}\,K$, attains at $\omega\sim 0$ the values rather big to force the enhancement factor to drop down to 0.5, thus doubling the $\mathrm{Im}\,R_{11}$ value. However, this value of $(1-W\,\mathrm{Re}\,K)_{11}$ is much higher than the value corresponding to the creation of spin waves with long lifetimes which is about 0.05, see Ref. 39.

In Fig. 10 we present the results of the *GW* and *GW+T* calculations for momentum-averaged lifetimes. As follows from Fig. 5, the highest energy of *d*-states in Pd is about 0.3 eV above Fermi level. The density of free-electron-like states at higher energy is much lower than the density of *d*-states. Therefore, the kernel's spectral function of electron-hole scattering, which depends on the convolution of the density of occupied and empty states, appears to be much bigger than the spectral function of the electron-electron scattering which can be approximated by the convolution of empty states. So we neglect the contribution of multiple electron-electron scattering in the lifetime calculations. As

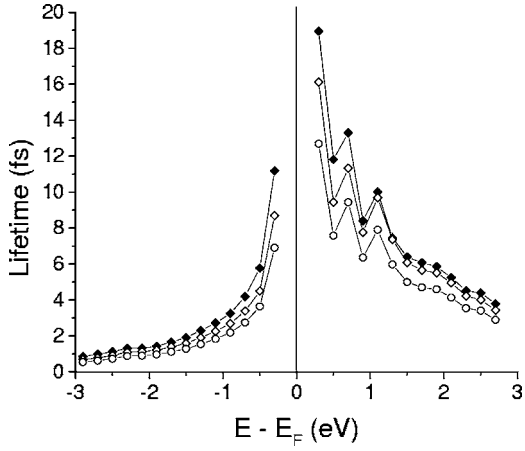

FIG. 10. Momentum-averaged electron and hole lifetimes in Pd. Black diamonds: Lifetimes within *GW* approach; open diamonds: Lifetimes within *GW+T* approach, including double-counting corrections; open circles: Lifetimes within *GW+T* approach without double-counting corrections.

follows from Fig. 10, the major contribution to the lifetimes belongs to the *GW* term, and the *T*-matrix contribution without DCT reduces the lifetimes by about 20%. The value of DCT appears to be about 50% of the *T*-matrix term, and the effect of the *T*-matrix with the subtracted DCT is to decrease the lifetimes by only about 10%. The smallness of the *T*-matrix effect in Pd is an unexpected result, taking into account that such effect in Ta with less correlated electron interactions is markedly bigger. Comparing the electron lifetimes in Pd with the hole lifetimes we find also a correspondence with the density of states. The hole lifetimes are governed by the density of 4*d*-states which is about four times higher than the density of free-electron-like electron excited states, so the hole lifetimes appear to be about four times less.[27] Noteworthy is that the averaged electron lifetimes in Pd, although associated with free-electron-like states, essentially differ from the values predicted by Fermi liquid theory.[27] The band-structure effects appear to be also important here. A simple model of the density of states convolutions with constant transition matrix element, based on the first-principle density of states, describes fairy well the energy dependence of the momentum-averaged lifetimes.[27]

B. Ta

In Fig. 11 we show the momentum and frequency dependence of the main matrix element of the electron-hole kernel's spectral function for Ta. At small q we observe a peak with the frequency about 0.5 eV. The maximum of the peak is 5 times less than that in Pd. Consequently it leads to smaller susceptibilities shown in Fig. 12. Nevertheless, the contribution of collective excitations described by the value R_T^{-+} is comparable with the contributions of the single excitations R_K^{-+}. This is due to the inverse enhancement factor $(1-W\,\mathrm{Re}\,K)_{11}$ that we show in Fig. 13 together with the main matrix elements of the kernel, $\mathrm{Im}\,K_{11}$ and $\mathrm{Re}\,K_{11}$. Since $\mathrm{Im}\,K=\pi S$, the $\mathrm{Im}\,K_{11}$ has a peak near 0.5 eV. The value $\mathrm{Re}\,K_{11}$, i.e., the Hilbert-transform of $\mathrm{Im}\,K_{11}$, is much smaller

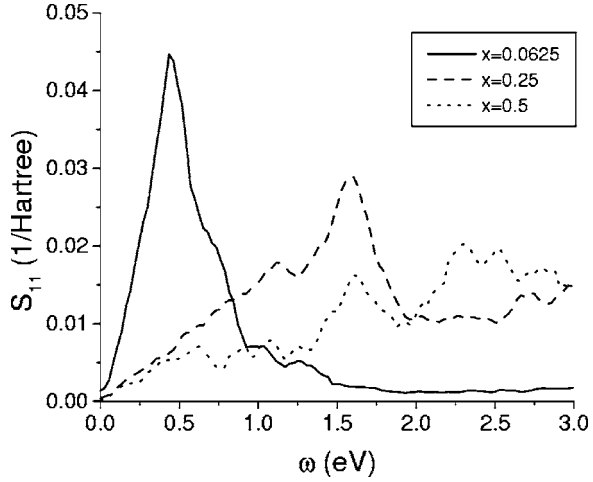

FIG. 11. Frequency dependence of the main matrix element S_{11} of Ta spectral function at $q=(2\pi/a)(x,0,0)$.

than that of Pd, so the static value of Re K_{11} in Ta appears to be about one order less. However, at zero frequency the values of $(1-W\,\mathrm{Re}\,K)_{11}$ in Ta and Pd are comparable. At low frequencies the changes in $(1-W\,\mathrm{Re}\,K)_{11}$ in Ta are small, and at 0.25 eV this matrix element is smaller by a factor of 2 than in Pd. Such a rather small value of the inverse enhancement factor in Ta is related with a much higher value of the screened potential W. For example, in Ta the matrix element W_{11} at $q=(2\pi/a)(0.05,0.05,0.0)$ is 3.45 Hartree units, and in Pd it is only 0.82 Hartree. So even with small K the product $(WK)_{11}$ appears to be big in Ta. We will show below that the static screened potential is the quantity important to also explain the differences between the values of the T-matrix self-energy terms in Pd, Ta, and Al.

In Fig. 14 we show the calculated and experimental data on electron and hole lifetimes in Ta. The calculations yield very small electron-electron and hole-hole self-energies, so we omit them. Also small, within 1 to 2 fs, are the double-counting corrections. Therefore, the T-matrix self-energy is

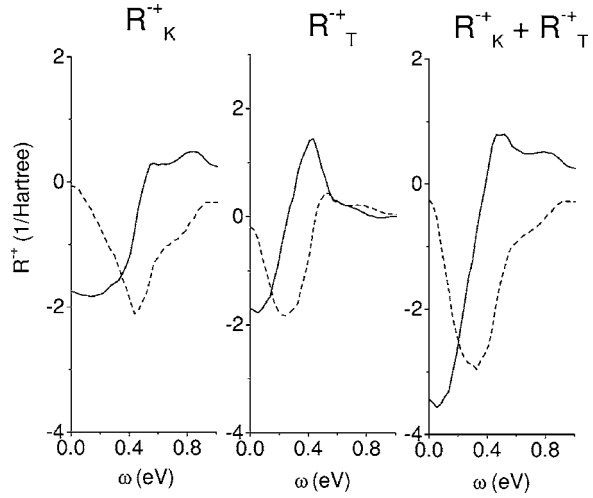

FIG. 12. Components of transverse susceptibility in Ta. Solid line: real part of R^{-+}; dashed line: Imaginary part of R^{-+}. $q=(2\pi/a)(0.0625,0,0)$.

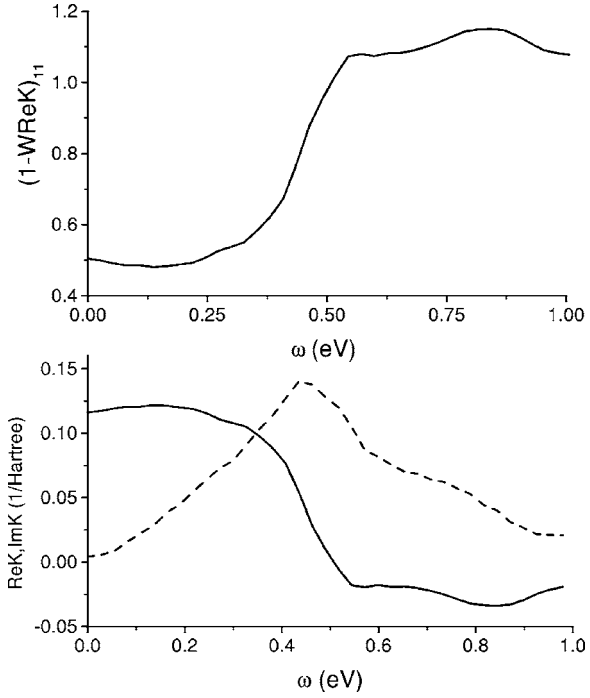

FIG. 13. Top panel: Frequency dependence of the main matrix element of the inverse enhancement factor $(1-WK)_{11}$ in Ta. Bottom panel: Imaginary part (dashed line) and real part (solid line) of the main matrix element of electron-hole kernel in Ta. $q=(2\pi/a)(0.0625,0,0)$.

mainly provided by the electron-hole scattering. The decrease of lifetimes appears to be about 30–40%. Within the inaccuracy of experimental data, which is evaluated in Ref. 49 as 2 fs, we have a good correspondence between the $GW+T$ and experimental results.

Remarkably, the T-matrix contribution to the quasiparticle self-energy in Ta appears to be bigger than in Pd, although Pd is a material with stronger electron correlations.

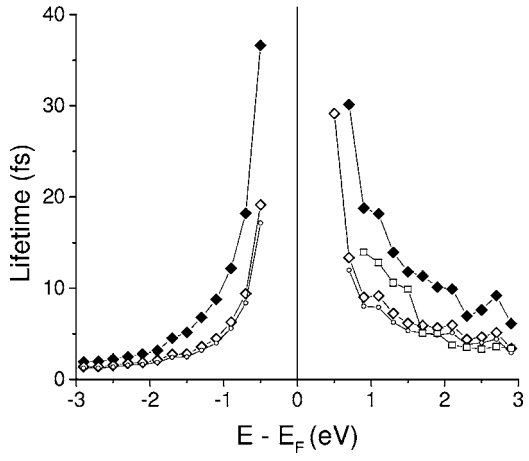

FIG. 14. Momentum-averaged electron and hole lifetimes in Ta. Black diamonds: Lifetimes within GW approach; open diamonds: Lifetimes within $GW+T$ approach, including double-counting corrections; small open circles: Lifetimes within $GW+T$ approach without double-counting corrections; open squares: experimental relaxation times in Ta, Ref. 42.

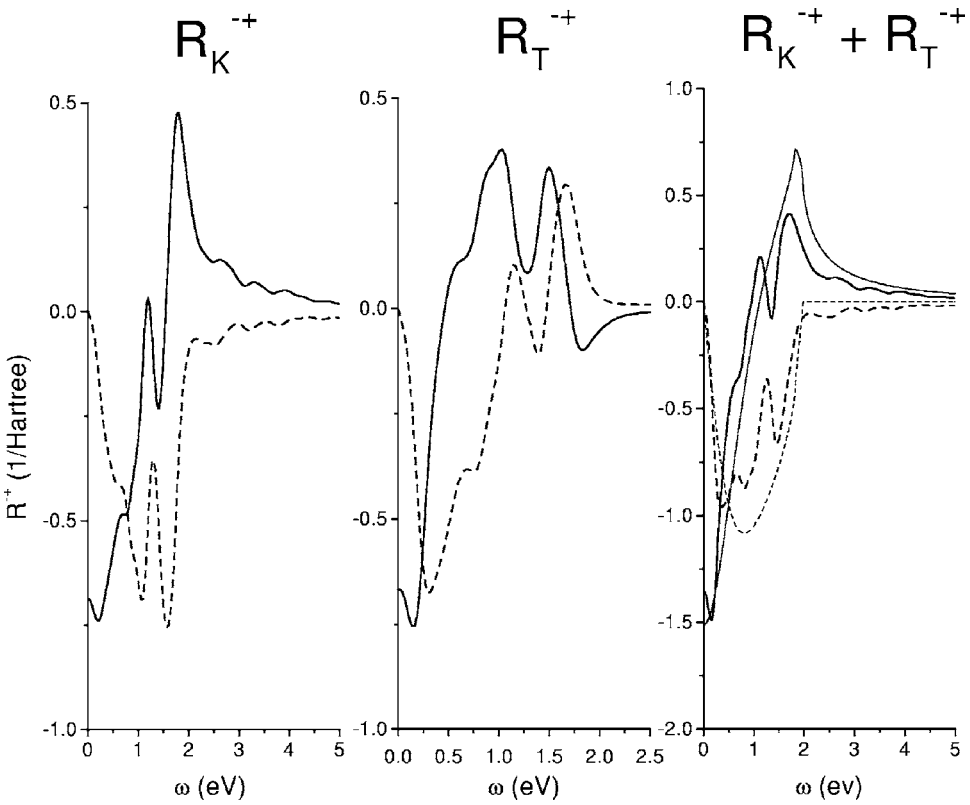

FIG. 15. Components of the transverse susceptibility in Al at $q=(2\pi/a)(0.05,0.05,-0.05)$. Thick solid line: real part of R^{-+}; thick dashed line: Imaginary part of R^{-+}. With thin solid (dashed) line in figure for R_K+R_T we show the Fermi liquid results at $r_s=2.0$.

We explain this by a higher value of the screened potential W in Ta, which provides higher T-matrix self-energy through Eqs. (22) and (26).

C. Al

Aluminum is a typical free-electron-like metal with relatively small and smoothly changing density of electron states, see Fig. 5. So we have a possibility to check our implementations by performing Fermi liquid theory (FLT) calculations for the self-energy and related values. Within FLT we calculate the GW term by means of Eq. (2), replacing the LDA wave functions with normalized plane waves and expressing $\mathrm{Im}\, W(\mathbf{q},\omega)$ through the RPA Lindhardt's dielectric function $\epsilon(\mathbf{q},\omega)$. In these calculations we employ dynamic potential $W(\mathbf{q},\omega)=\epsilon^{-1}(\mathbf{q},\omega)v$ with bare Coulomb potential $v=4\pi/\mathbf{q}^2$ (in Hartree units). This corresponds to the traditional FLT calculations,[18,33,59] and we extend FLT by including the T-matrix term. For nonmagnetic systems the kernel defined by Eq. (17) is equal to $K(\mathbf{q},\omega)=-P(\mathbf{q},\omega)/2=-(1-\epsilon(\mathbf{q},\omega))/(2v)$. As in our *ab initio* calculations, in FLT we employ static screened potential $W(\mathbf{q},0)$, so with ω-dependent K the T-matrix is

$$T(\mathbf{q},\omega)=\{1+\epsilon^{-1}(\mathbf{q},0)[1-\epsilon(\mathbf{q},\omega)]\}^{-1}\epsilon^{-1}(\mathbf{q},0)v(\mathbf{q}). \tag{40}$$

With the static screened potential the transverse susceptibility becomes

$$R^{-+}(\mathbf{q},\omega)=\{1+\epsilon^{-1}(\mathbf{q},0)[1-\epsilon(\mathbf{q},\omega)]/2\}[\epsilon(\mathbf{q},\omega)-1]/(2v). \tag{41}$$

The summation over one-particle states in the calculations for $\mathrm{Im}\,\Sigma$ is performed numerically. The Hilbert transform from the imaginary part of the self-energy to real part converges with a high limit of integration over frequency very slowly, and we have an inaccuracy in the evaluated Green's function re-normalization factor Z, Eq. (34). So we prefer to apply the value of the re-normalization factor $Z=0.75$ that follows from FLT calculations without Hilbert transform, Ref. 59, for the electron density parameter $r_s=2.0$.

In Fig. 15 we show the components of the transverse susceptibility for small momentum $\mathbf{q}$. Similarly to Pd and Ta, their imaginary parts have dips, but at much higher frequency. For the frequency smaller than 0.1 eV the magnitude of $\mathrm{Im}\, R$ is incomparably less than that in Pd, so the results for Al do not suppose the existence of low-temperature anomalies similar to those in Pd. The R_K and R_T contributions appear to be comparable in value, thus revealing the importance of multiple scattering for the dynamic susceptibility. The total static susceptibility is, however, six times less than in Pd. We also find a qualitative agreement between the transverse susceptibility calculated from first principles and from FLT.

In Fig. 16 we show the main matrix elements of the inverse enhancement factor $(1-W\,\mathrm{Re}\,K)_{11}$ and of real and imaginary part of kernel, $\mathrm{Re}\,K_{11}$ and $\mathrm{Im}\,K_{11}$. We see that, because of a small density of states, the kernel of Al is much smaller than in Pd, Ta, but the enhancement factor appears to be comparable with that in Pd and Ta.

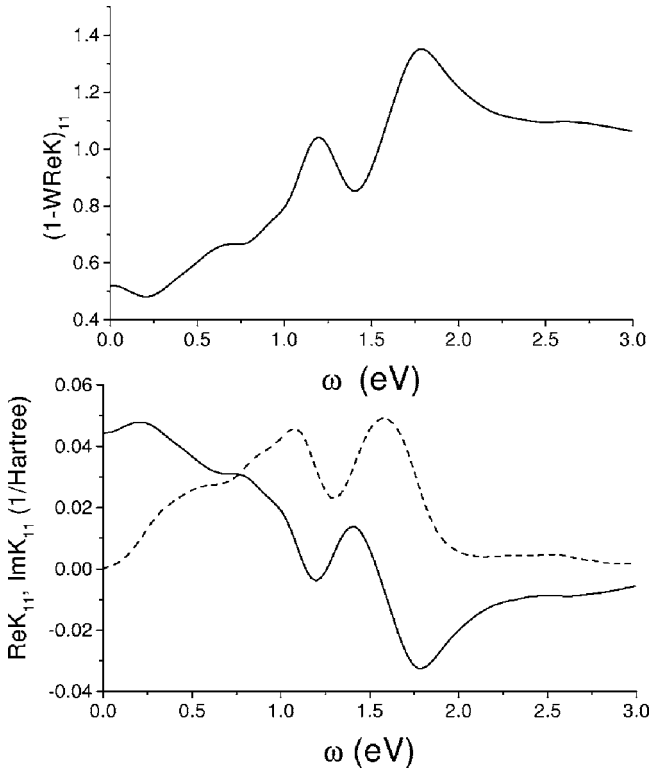

FIG. 16. Top panel: Frequency dependence of the inverse enhancement factor $(1-WK)_{11}$ for Al. Bottom panel: Imaginary part (dashed line) and real part (solid line) of the main matrix element of kernel in Al. $q=(2\pi/a)(0.05,0.05,0.05)$.

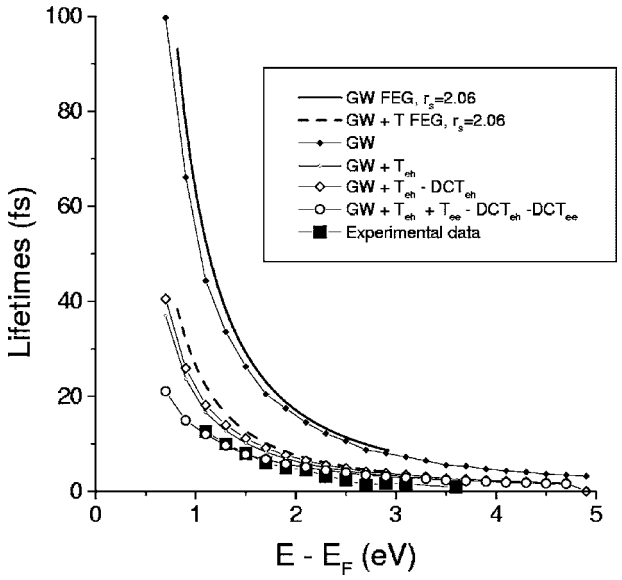

FIG. 17. Momentum-averaged electron lifetimes in Al. Solid diamonds: *ab initio GW* calculations; big open diamonds: *GW+T* calculations with included multiple electron-hole scattering and double counting term D(R); small open diamonds: *GW+T* calculations with included multiple electron-hole scattering and omitted double counting term; open circles: *GW+T* calculations with included multiple electron-hole and electron-electron scattering and double counting terms D(R), D(P); solid squares: Experimental data of Ref. 13 not corrected for cascade electrons and transport effects. Thick solid line represents the results of the Fermi-liquid theory, whereas thick dashed line corresponds to Fermi liquid theory with included multiple electron-hole scattering, see text.

We find that a small value of the inverse enhancement factor is caused by a very big value of the screened potential. At $\mathbf{q}=(2\pi/a)(0.05,0.05,0.05)$ we have the main matrix element $W_{11}=10.90$ Hartree. It is much higher than W_{11} in Ta and Pd (3.45 and 0.82 Hartree, respectively), so the product $(W\,\mathrm{Re}\,K)_{11}$ is for Al about 0.5.

Remarkably, the essential decrease of the screened potential from Al to Ta and Pd is well explained by the Thomas-Fermi theory for nonuniform media.[32] The dielectric function is expressed in this theory as $\epsilon(q)=1+(\lambda_s^2/q^2)$, where the screening wave vector λ_s is determined by the density of states at the Fermi level through $\lambda_s^2=4\pi N(E_F)$. The values of $N(E_F)$ for Al, Ta, Pd are 0.089, 0.268, and 0.735 $1/(\mathrm{Hartree}\times\mathrm{at.\,unit}^3)$, respectively. The corresponding λ_s values are 1.12, 3.36, and 9.23 at. units. For the screened potential we have in this theory $W(q)=1/[q^2/4\pi+N(E_F)]$. So at $q=0$ the values of the screened potential are 11.2, 3.7, and 1.36 Hartree, in good agreement with our first-principle values of W_{11}.

In Fig. 17 we demonstrate the calculated electron lifetimes in Al and compare them with available experimental data. Both the *GW* and *GW+T* results agree well with the data of the Fermi liquid theory. The *GW* momentum-averaged lifetimes are much higher than the experimental relaxation times obtained by means of the TR-2PPE spectroscopy, Ref. 13. The inclusion of multiple electron-hole scattering by means of the *T*-matrix theory significantly decreases the lifetimes. However, the lifetimes are still much higher than the experimental data. Including electron-electron scattering, we further decrease calculated lifetimes, and finally the *GW+T* lifetimes are close to experimental data.

We find a good correspondence between our results for Al and the calculations for lifetimes of positrons in metals[60] where an essential role of the *T*-matrix scattering has been shown. Note also that an essential reduction in the lifetimes, as compared with the data of the Fermi liquid theory, has been predicted in Ref. 61 based on the kinetic theory and the generalized mean-field theory.

Therefore, we see that in aluminum the increase of the decay rate because of the inclusion of multiple electron-hole scattering is bigger than in Pd and Ta, and the contribution of the decay rate due to the electron-electron scattering is comparable with that of the electron-hole scattering. We notice also that the neglecting of the double counting term D(R) changes the lifetimes by about 5% only. So in Al, as in Ta, the double-counting term is much smaller than the *GW* and *T*-matrix terms, and can be omitted.

IV. CONCLUSIONS

We have presented an *ab initio GW+T* approach for calculations of excited electron lifetimes. The method includes the evaluation of the first self-energy term within *GW* approximation and the higher terms within *T*-matrix approximation.

The *T*-matrix contributions in the decay rate of excited electrons are associated with the transverse spin susceptibility, so we have investigated the dynamic spin susceptibility in Pd, Ta, and Al. As expected, in the spectral function of susceptibility for Pd we find low-energy paramagnon peaks. At small momenta we also find peaks in the susceptibility for Ta and Al, but their frequency is higher and amplitude is much lower. Unexpectedly, we find that the enhancement factor of the susceptibility, i.e., the value $[1-WK]^{-1}$ describing the contribution of collective spin fluctuations, is comparable in magnitude in Pd, Ta, and Al. This is caused by the higher value of the screened potential in Al than in Ta and Pd.

The *T*-matrix self-energy includes electron-electron, hole-hole, and electron-hole contributions. The double-counting term in the *GW* and *T*-matrix has also to be considered. We estimate the role of all these terms for the calculations of the momentum-averaged lifetimes. One may expect that in Pd, a material with stronger electron correlations, the *T*-matrix electron-hole term should be bigger than in Ta and Al. However, we reveal an opposite trend: the reduction of the lifetimes due to the *T*-matrix is in Pd markedly smaller than in Ta and Al. So from Pd to Ta and Al we have due to the screened potential an increase in the imaginary part of the *T*-matrix self-energy which is accompanied by the decrease of lifetimes. Within the Thomas-Fermi theory for nonuniform media this change of screening can be associated with the change of the density of states at the Fermi level.

We find that the double-counting term is small in all the metals considered. The *T*-matrix electron-electron scattering term is much bigger in Al than in Pd and Ta. The inclusion of the electron-electron term in the self-energy of Al essentially reduces lifetimes, bringing them in better agreement with experimental data.

Although the *T*-matrix theory has been introduced originally to study the electronic properties of strongly correlated materials, our calculations show that the *T*-matrix effects can be important for the electron lifetimes in a broader range of materials with sufficiently strong screened potential. It would be interesting to apply the *GW+T* formalism to others paramagnetic and ferromagnetic systems.

ACKNOWLEDGMENTS

This work was partially supported by the University of the Basque Country, the Departamento de Educación del Gobierno Vasco, MCyT (Grant No. Mat 2001-0946), and the European Community 6th Network of Excellence NANOQUANTA (NMP4-CT-2004-500198).

[1] J. Bokor, Science **246**, 1130 (1989); R. Hight, Surf. Sci. Rep. **21**, 275 (1995).
[2] C. A. Schmuttenmaer, M. Aeschlimann, H. E. Elsayed-Ali, R. J. D. Miller, D. A. Mantell, J. Cao, and Y. Gao, Phys. Rev. B **50**, 8957 (1994).
[3] T. Hertel, E. Knoesel, M. Wolf, and G. Ertl, Phys. Rev. Lett. **76**, 535 (1996).
[4] S. Ogawa, H. Nagano, and H. Petek, Phys. Rev. B **55**, 10869 (1997).
[5] J. Cao, Y. Gao, R. J. D. Miller, H. E. Elsayed-Ali, and D. A. Mantell, Phys. Rev. B **56**, 1099 (1997).
[6] E. Knoesel, A. Hotzel, and M. Wolf, Phys. Rev. B **57**, 12812 (1998).
[7] E. Knoesel, A. Hotzel, T. Hertel, and M. Wolf, Surf. Sci. **368**, 76 (1996).
[8] J. Cao, Y. Gao, H. E. Elsayed-Ali, R. J. D. Miller, and D. A. Mantell, Phys. Rev. B **58**, 10948 (1998).
[9] M. Aeschlimann, M. Bauer, S. Pawlik, W. Weber, R. Burgermeister, D. Oberli, and H. C. Siegmann, Phys. Rev. Lett. **79**, 5158 (1997).
[10] R. Knorren, K. H. Bennemann, R. Burgermeister, and M. Aeschlimann, Phys. Rev. B **61**, 9427 (2000).
[11] W. Nessler, S. Ogawa, H. Nagano, H. Petek, J. Shimoyama, Y. Nakayama, and K. Kishio, Phys. Rev. Lett. **81**, 4480 (1998).
[12] M. Bauer, S. Pawlik, and M. Aeschlimann, Proc. SPIE **3272**, 201 (1998).
[13] M. Aeschlimann, M. Bauer, S. Pawlik, R. Knorren, and G. Bouzerar, Appl. Phys. A: Mater. Sci. Process. **71**, 485 (2000).
[14] F. Passek, M. Donath, K. Ertl, and V. Dose, Phys. Rev. Lett. **75**, 2746 (1995).
[15] H.-J. Drouhin, Phys. Rev. B **62**, 556 (2000).
[16] E. Zarate, P. Apell, and P.-M. Echenique, Phys. Rev. B **60**, 2326 (1999).
[17] J. M. Pitarke, V. P. Zhukov, R. Keiling, E. V. Chulkov, and P. M. Echenique, ChemPhysChem **5**, 1284 (2004).
[18] G. D. Mahan, *Many-particle Physics* (Plenum, New York, 1990).
[19] I. Campillo, V. M. Silkin, J. M. Pitarke, E. V. Chulkov, A. Rubio, and P. M. Echenique, Phys. Rev. B **61**, 13484 (2000).
[20] W.-D. Schöne, R. Keyling, M. Bandić, and W. Ekardt, Phys. Rev. B **60**, 8616 (1999).
[21] V. P. Zhukov and E. V. Chulkov, J. Phys.: Condens. Matter **14**, 1937 (2002).
[22] I. Campillo, J. M. Pitarke, A. Rubio, E. Zarate, and P. M. Echenique, Phys. Rev. Lett. **83**, 2230 (1999).
[23] F. Ladstädter, U. Hohenester, P. Puschnig, and C. Ambrosch-Draxl, Phys. Rev. B **70**, 235125 (2004).
[24] R. Keyling, W.-D. Schöne, and W. Ekardt, Phys. Rev. B **61**, 1670 (2000).
[25] V. P. Zhukov, F. Aryasetiawan, E. V. Chulkov, I. G. de Gurtubay, and P. M. Echenique, Phys. Rev. B **64**, 195122 (2001).
[26] I. Campillo, A. Rubio, J. M. Pitarke, A. Goldmann, and P. M. Echenique, Phys. Rev. Lett. **85**, 3241 (2000).
[27] V. P. Zhukov, F. Aryasetiawan, E. V. Chulkov, and P. M. Echenique, Phys. Rev. B **65**, 115116 (2002).
[28] M. R. Bacelar, W.-D. Schöne, R. Keyling, and W. Ekardt, Phys. Rev. B **66**, 153101 (2002).
[29] F. Ladstädter, P. F. de Pablos, U. Hohenester, P. Puschnig, C. Ambrosch-Draxl, P. L. de Andres, F. García-Vidal, and F. Flores, Phys. Rev. B **68**, 085107 (2003).
[30] L. Hedin and S. Lundqvist, in *Solid State Physics*, edited by H.

Ehrenreich, F. Seitz, and D. Turnbull (Academic, New York, 1969), Vol. 23, p. 1.
[31] F. Aryasetiawan, in *Strong Coulomb Correlations in Electronic Structure Calculations*, edited by V. I. Anisimov (Gordon and Breach, Singapore, 2001).
[32] J. C. Inkson, *Many-body Theory of Solids* (Plenum, New York, 1984).
[33] A. L. Fetter and J. D. Walecka, *Quantum Theory of Many-particle Systems* (McGraw-Hill, New York, 1971).
[34] J. Kanamory, Prog. Theor. Phys. **30**, 275 (1963).
[35] D. R. Penn, Phys. Rev. Lett. **42**, 921 (1979).
[36] A. Liebsch, Phys. Rev. B **23**, 5203 (1981).
[37] H. Yasuhara, H. Suchiro, and Y. Ousaka, J. Phys. C **21**, 4045 (1988).
[38] J. Hong and D. L. Mills, Phys. Rev. B **59**, 13840 (1999).
[39] K. Karlsson and F. Aryasetiawan, Phys. Rev. B **62**, 3006 (2000).
[40] M. Springer, F. Aryasetiawan, and K. Karlsson, Phys. Rev. Lett. **80**, 2389 (1998).
[41] V. P. Zhukov, E. V. Chulkov, and P. M. Echenique, J. Magn. Magn. Mater. **272-276**, 466 (2004).
[42] V. P. Zhukov, E. V. Chulkov, and P. M. Echenique, Phys. Rev. Lett. **93**, 096401 (2004).
[43] P. M. Echenique, R. Berndt, E. V. Chulkov, Th. Fauster, A. Goldmann, and U. Höfer, Surf. Sci. Rep. **52**, 219 (2004).
[44] F. Aryasetiawan and O. Gunnarsson, Rep. Prog. Phys. **61**, 237 (1998).
[45] R. M. Dreizler and E. K. U. Gross, *Density Functional Theory* (Springer, New York, 1990).
[46] P. M. Echenique, J. M. Pitarque, E. V. Chulkov, and A. Rubio, Chem. Phys. **251**, 1 (2000).
[47] I. G. Gurtubay, J. M. Pitarke, and P. M. Echenique, Phys. Rev. B **69**, 245106 (2004).
[48] O. K. Andersen, O. Jepsen, and M. Sob, in *Electronic Band Structure and its Applications, Vol. 283 of the Lecture Notes in Physics*, edited by M. Yussouff (Springer, Heidelberg, 1987).
[49] V. P. Zhukov, O. Andreyev, D. Hoffman, M. Bauer, M. Aeschlimann, E. V. Chulkov, and P. M. Echenique, Phys. Rev. B **70**, 233106 (2004).
[50] J. F. Janak, Phys. Rev. B **16**, 255 (1977).
[51] M. M. Sigalas and D. A. Papaconstantopoulos, Phys. Rev. B **50**, 7255 (1994).
[52] S. Doniach and E. H. Sonderheimer, *Green's Functions for Solid State Physisists* (Imperial College Press, London, 1999).
[53] P. Mohn and K. Schwarz, J. Magn. Magn. Mater. **104**, 685 (1992).
[54] B. Kirchner, W. Weber, and J. Voitländer, J. Phys.: Condens. Matter **6**, 2603 (2994).
[55] E. Stenzel and H. Winter, J. Phys. F: Met. Phys. **16**, 1789 (1986).
[56] A. G. Eguiluz, A. Fleszar, and J. A. Gaspar, Nucl. Instrum. Methods Phys. Res. B **96**, 550 (1995).
[57] S. Y. Savrasov, Phys. Rev. Lett. **81**, 2570 (1998).
[58] F. Aryasetiawan and K. Karlsson, Phys. Rev. B **60**, 7419 (1999).
[59] B. I. Lundqvist, Phys. Status Solidi **32**, 273 (1969).
[60] C. Zhang, N. Tzoar, and P. M. Platzman, Phys. Rev. B **37**, 2401 (1988).
[61] I. Nagy, J. I. Juaristi, and P. M. Echenique, Phys. Rev. B **63**, 035102 (2000); I. Nagi, M. Alducin, and P. M. Echenique, *ibid.* **65**, 235102 (2002).